
Article:
Castanheira-Pinto, A, Fernández-Ruiz, J, Colaço, A et al. (2022) A simplified approach for predicting the non-linear critical speed of railway tracks. Transportation Geotechnics, 37. 100865. ISSN: 2214-3912

https://doi.org/10.1016/j.trgeo.2022.100865

A SIMPLIFIED APPROACH FOR PREDICTING THE NON-LINEAR CRITICAL SPEED OF RAILWAY TRACKS

Alexandre Castanheira-Pinto[1,*], Jesus Fernández Ruiz [2], Aires Colaço[1], Pedro Alves Costa[1] and David P. Connolly[3]

[1] *Construct-FEUP, University of Porto, Porto, Portugal*
[2] *University of La Coruña, Department of Civil Engineering, La Coruña, Spain*
[3] School of Civil Engineering, University of Leeds, UK

ABSTRACT

When trains approach the railway track-ground critical speed ground deformations are amplified, potentially exceeding the linear-elastic strain range in the supporting earthworks. This leads to non-linear soil behavior which can be difficult to model due to high computational cost and the need for detailed characterization of soil properties. As a solution, for the first time this research presents a simplified methodology to calculate the non-linear critical speed of track-ground structures. The methodology uses a novel semi-analytical approach that combines dispersion curves with a simplified linear equivalent model. Using the approach, a track-ground static strain field is first calculated, and then converted into a dynamic one using a non-dimensional dynamic amplification function, independent of the elastic properties of the soil. The result allows the non-linear critical speed to be calculated using static simulation results which are relatively straightforward to generate. The methodology is validated using a 3D non-linear HSSmall numerical model and then a parametric study is used to compare results for both concrete slab and ballasted tracks. The results show the proposed approach is a reliable tool for predicting the non-linear critical speed.

KEYWORDS: Simplified railway dynamics methodology; Non-linear critical speed; Railway dispersion curve technique; Non-dimensional dynamic amplification functions; Railway track dynamics, Railroad geodynamics

1 – INTRODUCTION

When high-speed railway lines are designed or upgraded, some track sections may be susceptible to dynamic amplification of vibration and track movement. This can cause environmental impacts, railway safety problems [1] and degradation of the geomechanical properties of the embankment and the foundation soils. These situations occur when the speed of the train is similar to that of the waves propagating in the ground, and is better known as the critical speed [2-6]. By definition, critical speed

is the velocity of the moving non-oscillating load that leads to maximum amplification of the dynamic response.

Due to the practical interest and importance of this problem, different methods for calculating the critical speed have been proposed in recent years, ranging from analytical [2-5, 7] to advanced numerical models [8-16]. Although the latter are more powerful and versatile, their computational cost is high and their applicability for practical engineering can be costly. In order to provide simpler and more practical tools, analytical methods based on wave propagation theory have recently been presented. This includes one proposed by Alves Costa et al. [3], inspired by studies presented in Sheng et al. [5], in which the critical speed is calculated by analysing the dispersive characteristics of the embankment-ground system and the bending wave propagation in the track. Using this low computational cost methodology and comparing the results against a 2.5D FEM-BEM model, the maximum difference is in the range 3-5%.

In the aforementioned numerical and analytical models, linear elastic behaviour of the soil is assumed. However, the critical speed is typically characterized by an increase in the strains in the embankment and supporting soils [16-20], possibly exceeding the linear elastic strain range of . For example, Fernández-Ruiz et al. [16], Alves Costa et al. [18], Dong et al. [19] and Shih et al. [20, 21], among others, have shown how non-linear models yield values of critical speed that are significantly lower (between 10-30%) than the linear elastic model, being more in line with experimental measurements [16, 18-20]. At the same time, Fernández-Ruiz et al [16] have shown how the effect of non-linearity is strongly affected by the type of track (ballasted or slab track) and the Plasticity Index (PI) of the soil foundation. These non-linearity studies are based on the shear modulus degradation and damping curves proposed by Ishibashi and Zhang [22].

Although truly non-linear constitutive models may be useful for studying the critical speed phenomenon [16, 20, 23, 24], their computational cost is high, in addition to requiring a very thorough characterization of soil properties. In this sense, a linear equivalent analysis improves computational efficiency and requires only the elastic properties of the soil, its PI and the mean effective stress (p') for its application [25-29]. It has been successfully applied in several critical speed investigations [18-20]. Shih et al [20] presents a comparison with a non-linear model, showing similar results for locations near the track. In these studies, an iterative process is applied to approximate non-linear behavior, starting by calculating an effective shear strain that is used to calculate updated values of shear modulus (G) and damping through degradation curves. Applying the updated value of the G modulus, the shear strain is recalculated and this process is repeated until the difference between the shear modulus in two successive iterations is below a pre-established tolerance. In this iterative process, the

effective shear strain is normally expressed as a percentage of the octahedral shear strain [18-20], which takes values between 0.2 (20%) and 1 (100%) [20, 30, 31].

Although the equivalent linear approach is simpler and more efficient than non-linear constitutive models, it still carries a higher computational cost compared to simple linear models. Thus, from a practical engineering point of view, this can make it unviable. Hence, the aim of this research is to present and validate a simplified methodology to predict the critical speed considering non-linear soil behaviour, starting from the static stress-strain field considering a linear elastic model. The proposed method combines an analytical track dispersion curve methodology with a simplified equivalent linear approach for the earthworks. Firstly the proposed steps comprising the simplified methodology to predict the non-linear critical speed are presented. Then, a dynamic amplification is defined to convert the static shear strains into dynamic ones. Finally, for both ballast and slab tracks, validation examples are used to compare against an alternative numerical approach.

2 – SIMPLIFIED METHODOLOGY TO PREDICT THE NON-LINEAR CRITICAL SPEED

The simplified methodology is based on a dispersion curve method considering the degraded properties of the embankment and the soil. It uses an analytical procedure to compute the critical speed, considering both the P-SV wave dispersion relationship of the soil and of the track. In this sense, by intersecting the soil and track dispersion curves the critical speed can be approximated as shown in the previous works [3, 16, 32]. The degradation of the geotechnical properties is calculated by means of a simplified linear equivalent analysis using the G degradation curves, considering the dynamic octahedral shear strain. This latter is derived from a static analysis being converted into the dynamic one by means of a dynamic amplification function. To better clarify the reader on the procedures which composed the simplified methodology a step-by-step approach is further presented.

2.1 –STEP 1: DETERMINE THE AVERAGE STATIC OCTAHEDRAL SHEAR STRAIN WITH DEPTH

First the simplified methodology computes the static octahedral shear strain with depth. To do so a static numerical model is used to obtain the Cartesian strains for the cross section where the load is applied, as expressed in Figure 1a). For that section, the average Cartesian strains are only computed for an area beneath the embankment where non-linear effects are dominant [16] (Figure 1b).

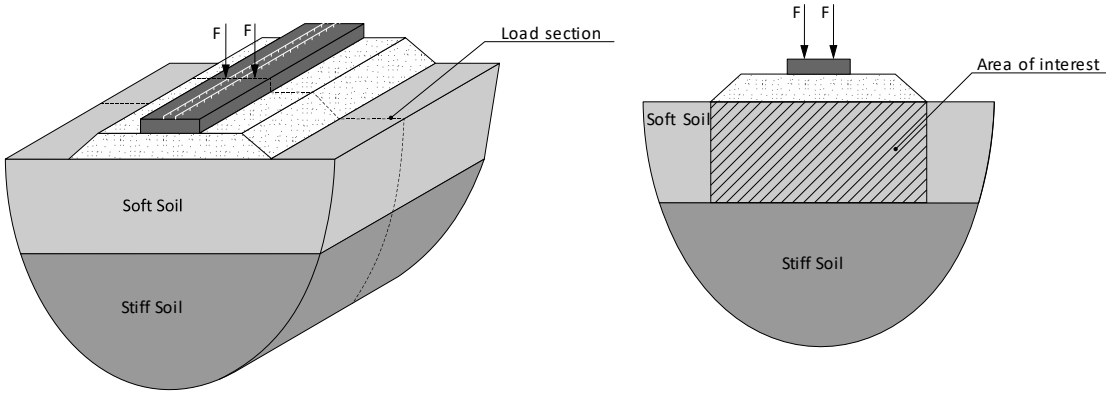

a) b)

Figure 1 – Scheme of operations of simplified methodology.

Using the Cartesian strains the average static octahedral shear strain with depth equation (1) is:

$$\gamma_{oct} = \frac{1}{3}\sqrt{\left(\varepsilon_x - \varepsilon_y\right)^2 + \left(\varepsilon_x - \varepsilon_z\right)^2 + \left(\varepsilon_y - \varepsilon_z\right)^2 + 6\cdot\left(\gamma_{xy}{}^2 + \gamma_{xz}{}^2 + \gamma_{yz}{}^2\right)} \quad (1)$$

where γ_{oct} is the octahedral shear strain, ε the Cartesian strains and γ the shear strain. It should be highlighted that the static octahedral shear strain could be computed by both a numerical method or an analytical solution.

2.2 – Step 2: Determine the average dynamic octahedral shear strain with depth

After calculating the average static octahedral shear strains, (e.g. Figure 2a) the dynamic octahedral shear strains expected at the critical speed are computed. To do so, the static octahedral shear strain is multiplied by a dynamic amplification function (Ω). This function is described later in this paper. Figure 2 shows a schematic illustration of the conversion procedure, where the average static octahedral shear strain (Figure 2a) is multiplied by the dynamic amplification function (Figure 2b) to obtain the dynamic octahedral shear strain (Figure 2c).

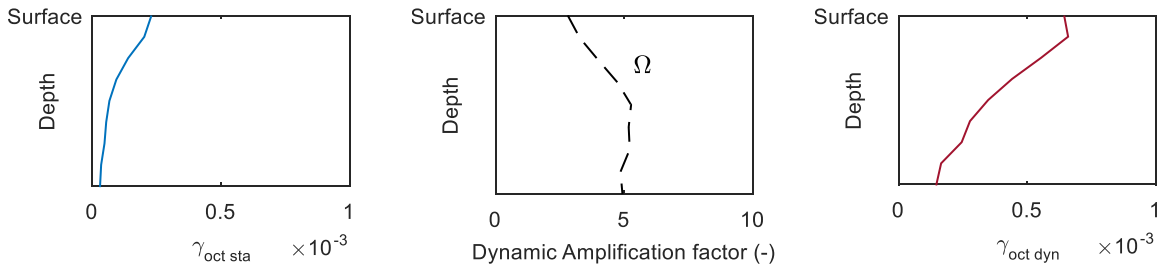

a) b) c)

Figure 2 – Schematic illustration of: a) static octahedral shear strain; b) dynamic amplification function (Ω); c) dynamic octahedral shear strain;

2.3 –STEP 3: DEGRADE THE ELASTIC LINEAR PROPERTIES

To simulate the degradation pattern in the soil domain, with the aim of predicting the non-linear critical speed, an approximate process is used. For each dynamic octahedral shear strain (Figure 2c), a shear modulus degradation percentage is estimated using an iterative procedure:

1. For a given dynamic octahedral shear strain, assess the corresponding value of G/G_0 using the Ishibashi backbone curves (Figure 3)

2. Update the previous octahedral shear strain using equation (2):

$$\gamma_{i+1} = \frac{\gamma_i}{G/G_0} \tag{2}$$

3. Repeat steps 1 and 2 until a convergence criteria is reached (e.g. error = 3%)
4. Compute the degraded elastic properties of the soil thickness using equation (3):

$$c_d = \sqrt{G/G_0} \cdot c \tag{3}$$

where c_d is the reduced wave velocity, G is the secant modulus, G_0 is the shear modulus at small strains, and c is the wave velocity of the soil layer under consideration.

Figure 3 shows an example representation of the procedure for a single value of dynamic octahedral shear strain. The iterative procedure is applied to several points with depth in order to capture the degradation pattern, being established by the authors as a good rule of thumb layers with 1m of thickness.

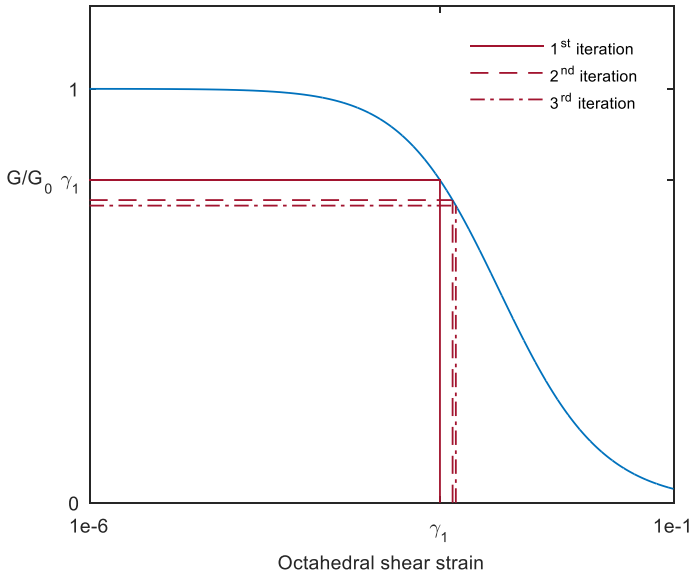

Figure 3 – Example computation of the degradation process using Ishibashi backbone curves

2.4 – STEP 4: PREDICT THE NON-LINEAR CRITICAL SPEED

Finally, the dispersion curve of the soil/earthworks (see Appendix B) is computed using the previously calculated degraded properties. The critical speed is given by the intersection point of the independent track and ground dispersion curves (Figure 24). An example of the process is shown in Figure 4 for a slab railway track. In should be highlighted that the same process is applied regardless of whether the track is at-grade or on an embankment.

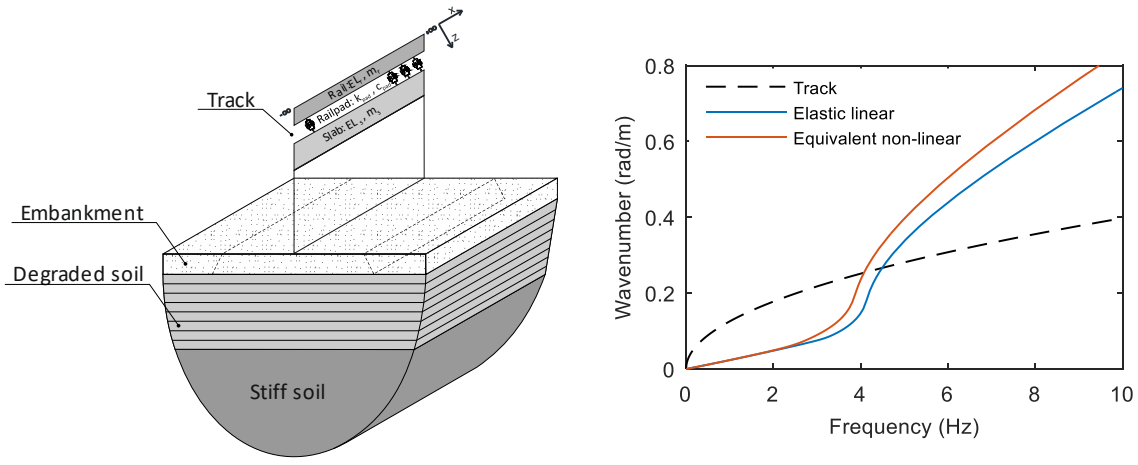

a) b)

Figure 4 – Scheme to determine the degradation dispersion curves and critical speed: a) degraded profile used to compute the dispersion curve; b) dispersion curves

3 – DYNAMIC AMPLIFICATION FUNCTION

3.1. GENERALITIES

The dynamic amplification function (Ω) from step 2 of the methodology relates the dynamic octahedral strains (i.e. those expected at th linear elastic critical speed) with the static octahedral strains expected at low speed. To determine this function, a 3D numerical model was used to compute the dynamic octahedral shear strain at the critical speed ($\gamma_{oct\,dyn}$) and for the static one ($\gamma_{oct\,sta}$), considering linear elastic behavior. In order to find a dynamic amplification function which could be applicable to commonly found soft soils. Since the dynamic response of an embankment and at-grade soil is different, separate functions are proposed. Therefore, firstly the dynamic amplification function for the soil (Ω_S) is presented, both for slab tracks and ballasted track, considering a homogeneous soil and a layered case. Secondly, the dynamic amplification function for the embankment (Ω_E) is presented.

3.2. DYNAMIC AMPLIFICATION FUNCTION FOR THE SOIL FOUNDATION (Ω_S)

3.2.1. Homogeneous soils

Three homogenous soil scenarios are studied, with C_s values of 80, 100 and 120 m/s, both for a conventional slab (Figure 5) and ballasted track (Figure 6). The elastic properties of the tracks and earthworks are shown in Table 1. The numerical model is developed in Plaxis [33] considering an axle load of 180 kN, details of which are in Fernández-Ruiz et al. [16]. The dynamic amplification factor found ($\gamma_{oct\,dyn} / \gamma_{oct\,sta}$) in the soil is shown in Figure 7.

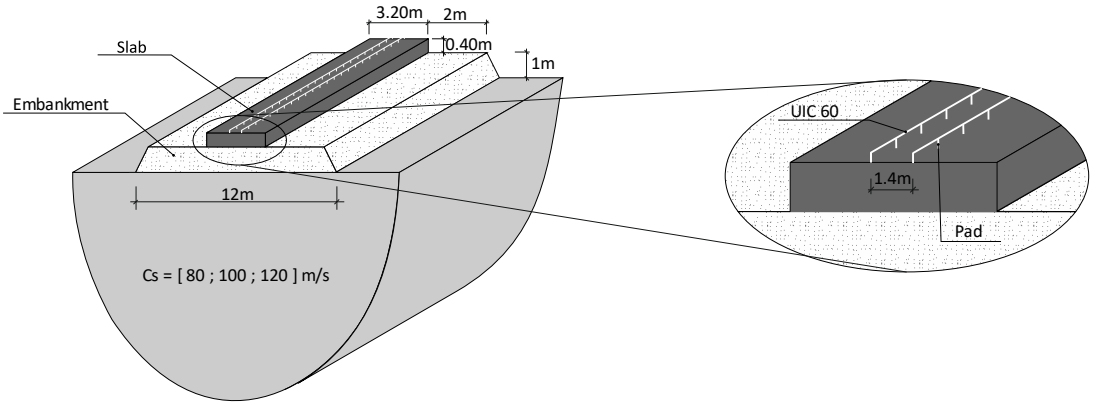

Figure 5 - Slab track scenarios for computing the dynamic amplification function (Ω_S)

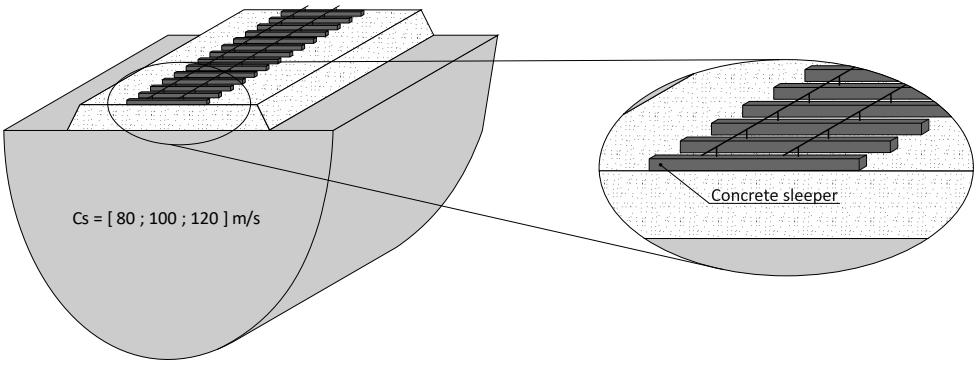

Figure 6 - Ballasted track scenarios for computing the dynamic amplification function (Ω_S)

Table 1 – Elastic material properties adopted

Layer	E (MPa)	ρ (Kg/m^3)	ν (-)	ξ (-)	Cs (m/s)
Slab/Sleeper	25e3	2500	0.20	0.01	2236
Embankment	200	2000	0.30	0.03	196
Soft soil	30.5/43.2/63.4	1600	0.35	0.03	80/100/120
Rail (UIC 60)	210e3	7850	0.30	0.01	5170
Rail pads	K_{pad}= 50 kN/mm, C_{pad}= 1.2x10^5 Ns/m^2 and 0.6 m of longitudinal spacing				

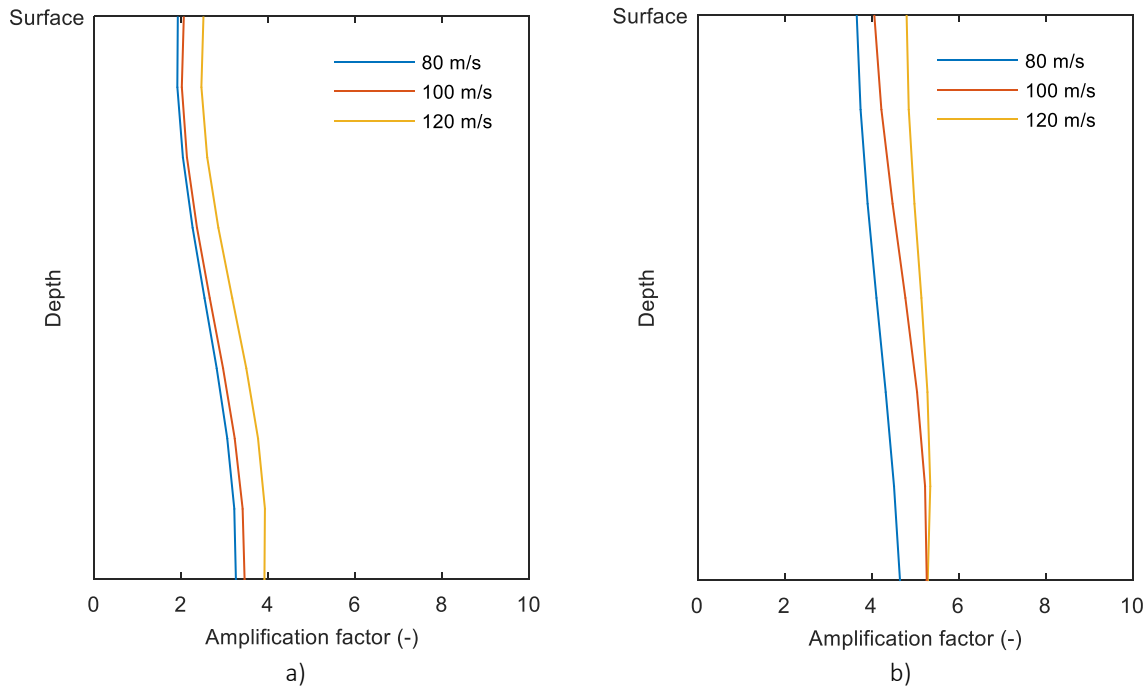

Figure 7 - Dimensional amplification factor for homogeneous cases: a) slab track; b) ballasted track

Considering the results, the dynamic amplification factor increases with C_s and also with depth for both track systems. Also, the dynamic amplification is higher in ballasted tracks. However, the form of the dynamic amplification factor is similar for the cases studied and for each track system, so the possibility of finding a non-dimensional coefficient that causes the differences between the cases to be minimal is studied. Thus, the following non-dimensional coefficient, hereafter named Stiffness Ratio (SR), is proposed:

$$SR = \frac{1}{\sqrt{\frac{C_{s_{soil}}}{C_{s_{embakment}}}}} \tag{4}$$

Applying this non-dimensional coefficient to the numerical results shown in Figure 7 gives the results in Figure 8, where it can be observed that the differences found in the 3 cases are minimal for both slab and ballasted tracks. It can also be observed in Figure 8 that the values of the non-dimensional amplification factor can be approximated as a straight line, which is a function of the depth and the bending stiffness of the track (EI). This value is the bending stiffness of two rails and slab for slab tracks, and only the bending stiffness of the two rails for ballasted tracks.

This fact is of great relevance because it enables the dynamic octahedral strain field (for the critical speed) to be found by means of a simple static analysis for any C_s value of soft soil. It is also noteworthy to highlight that the non-dimensional amplification function is the same for both track systems, only modifying the bending stiffness of the track.

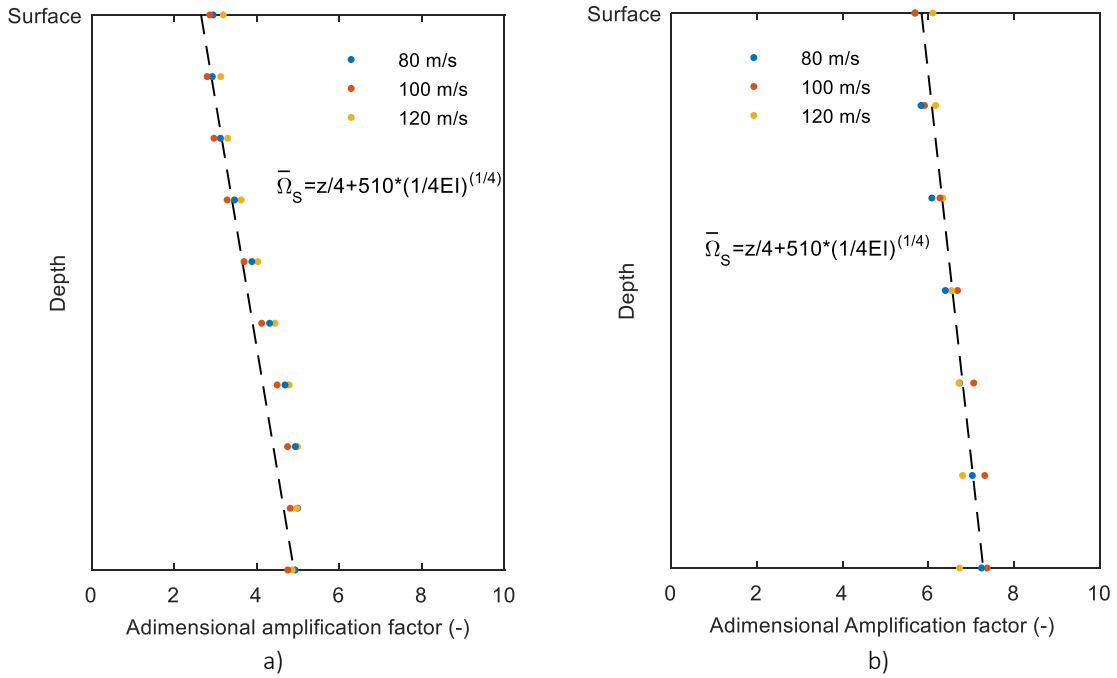

Figure 8 – Non-dimensional amplification factor for homogeneous cases: a) slab track; b) ballasted track

To convert the non-dimensional dynamic amplification function to a given scenario equation (5) is applied:

$$\Omega_s = \frac{\overline{\Omega}_s}{SR} \tag{5}$$

3.2.2. Layered soils

The preceding section showed how to find the dynamic strain state (at the critical speed) using static analysis for homogenous soils. However, in engineering practice, stratified geotechnical profiles are more common. As previously mentioned, a dynamic amplification function (Ω_s) is studied for stratified cases only for slab tracks since for ballasted tracks the non-linear speed is mainly influenced by the soil beneath the embankment [16]. To do this, three scenarios for slab tracks are considered, corresponding to soft soil thicknesses of 2, 4 and 8 meters, sitting on a stiff soil with C_s =200 m/s. These scenarios are shown in Figure 9, where the C_s value of the soft soil is 100 m/s.

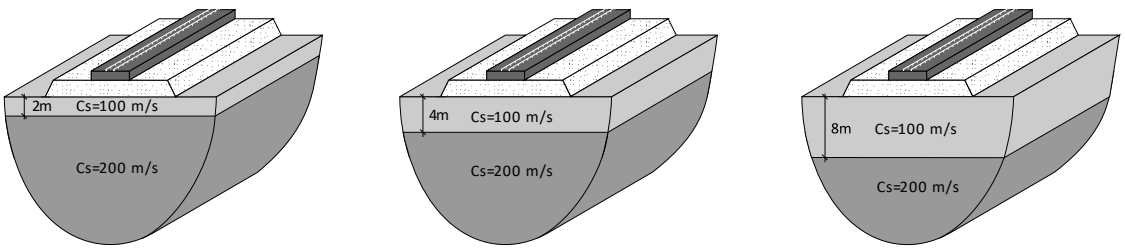

a) b) c)

Figure 9 - Layered scenarios: a) 2 m of soft soil; b) 4 m of soft soil; c) 8 m of soft soil.

The numerical results are shown in Figure 10a, where considerable differences can be observed as a function of the thickness of the soft soil. If a new coefficient, complimentary to the Stiffness Ratio (SR), is now applied to take into account the thickness of the soft soil, named Thickness Ratio (TR) (equation (6)), the results shown in Figure 10b are obtained.

$$TR = 1 + \frac{1}{\sqrt[3]{\left(\frac{1}{H_{soft_{soilt}}}\right)^2}} \tag{6}$$

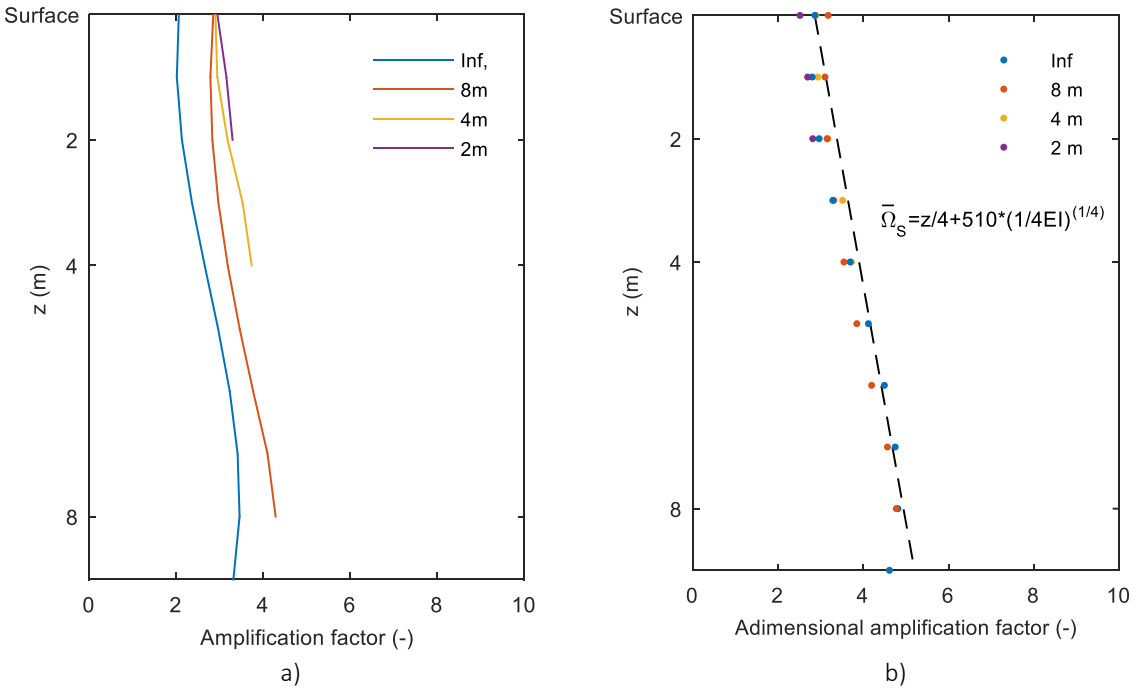

Figure 10 – Amplification factor for layered cases in slab track: a) Dimensional; b) Non-dimensional

It is observed that the fit with the non-dimensional amplification function obtained for homogeneous scenarios ($\overline{\Omega}_s$) is also acceptable for layered profiles. Combining the non-dimensional amplification function ($\overline{\Omega}_s$) and the correction coefficients (SR and TR) with the dynamic amplification function (Ω_s) a unifying relationship is defined as shown in equation (7):

$$\Omega_s = \frac{\overline{\Omega}_s}{(SR \times TR)} \tag{7}$$

3.3. Dynamic Amplification Function in the embankment (Ω_E)

3.3.1. Slab tracks scenarios

To study the dynamic amplification functions for the embankment (Ω_E) that give support to slab tracks, the same procedure is followed as before, but since this has a small thickness (1m), a single value of dynamic amplification is considered. The same cases analyzed above are studied, considering 4 thicknesses of soft soil (2, 4, 8m and homogeneous) for each of the 3 cases of S-wave propagation speed. This results in a total of 12 cases. The numerical results are shown in Figure 11, in which it can be seen that the dynamic amplification factor is almost independent of the soft soil C_s. However, there is a strong dependence on the thickness of the soft soil, showing how the dynamic amplification factor decreases with an increase in the thickness of the soft soil. Figure 11 also shows the interpolation function, which depends only on the thickness of the soft soil (h), and whose fit with the numerical results obtained is strong.

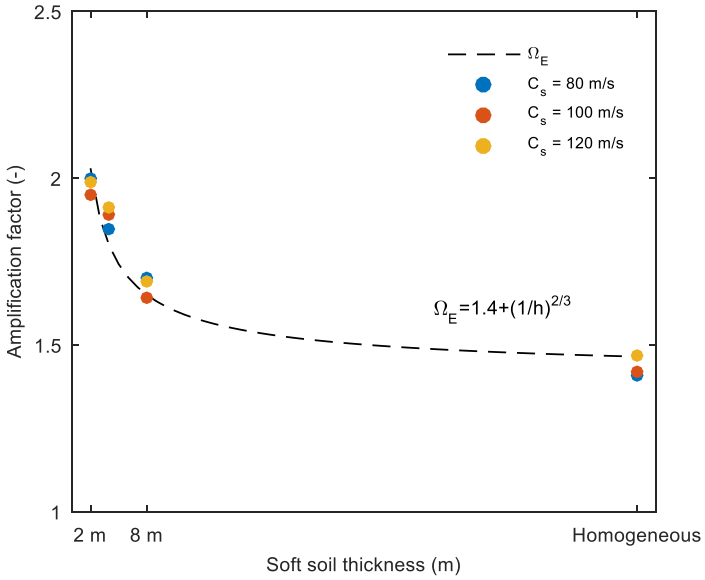

Figure 11 – Real and interpolated dynamic amplification factor for slab tracks on embankment

3.3.2. Ballasted tracks scenarios

The embankment dynamic amplification factor is also studied for ballasted tracks. As previously mentioned, only homogeneous cases are studied resulting in a total of 3 cases. The numerical results are shown in Figure 12 where it can be observed how this factor is adjusted using a linear function. Hence, C_s is known, the value of the dynamic octahedral shear strain can be obtained using the static values, simply by applying the dynamic amplification function used for the embankment (Ω_E).

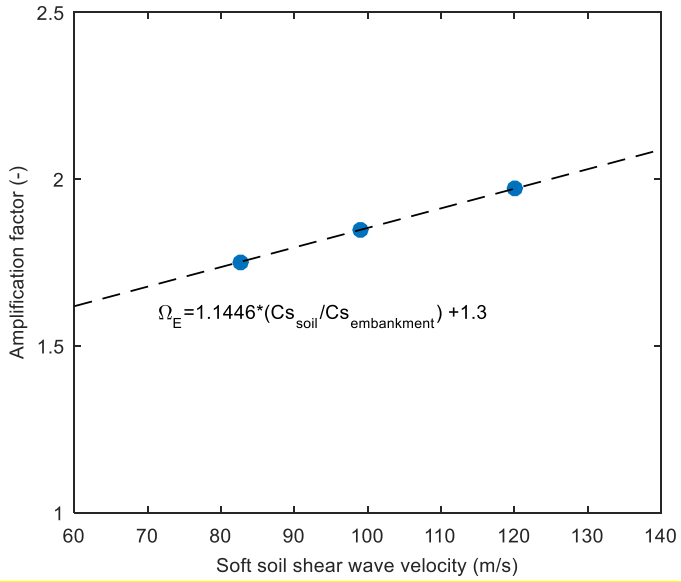

Figure 12 – Real and interpolated dynamic amplification factor for embankment in ballasted tracks.

4 – SIMPLIFIED METHODOLOGY VALIDATION

4.1. INTRODUCTION

To validate the simplified methodology first the slab track is considered, followed by the ballasted track. For each two scenarios are studied:

i) Validation case - a geotechnical scenario used to develop the dynamic amplification functions;

ii) Application case, - a geotechnical scenario with unseen properties.

For all cases validation is achieved by comparing the results from proposed methodology against a 3D non-linear FEM analysis performed in the time domain (Plaxis), as shown in Figure 13.

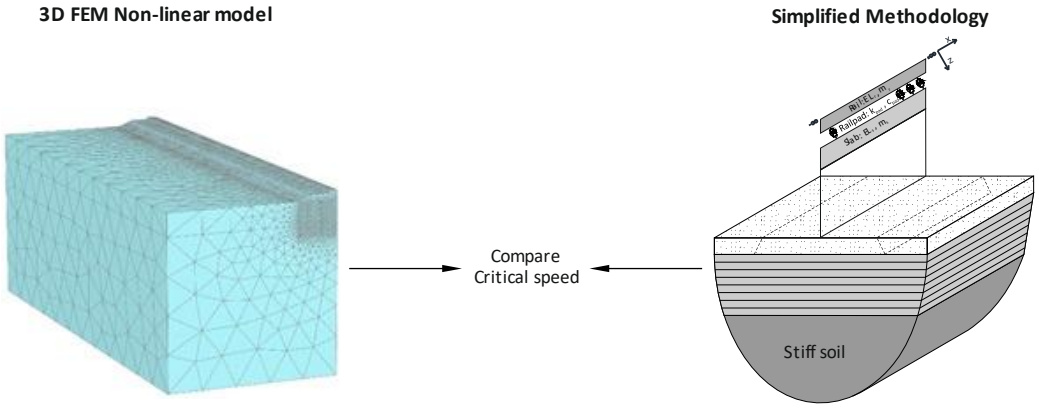

Figure 13 – Simplified methodology validation scheme

4.2. SLAB TRACK

4.2.1 Validation case

The critical speed is evaluated for one of the geotechnical scenarios considered in the adjustment outlined in section 3, using both the simplified methodology and the 3D FEM numerical model. The case is shown in Figure 9c and the elastic properties of the track and soil are shown in Table 1. The geotechnical profile is made up of the two soils, one soft with thickness 8 m and C_s = 80 m/s, and one stiff (C_s = 200 m/s) of indefinite depth, as described above. In order to validate the simplified methodology a comparison must be established with a numerical model capable of simulating the non-linear behaviour of the soil (Plaxis). For the constitutive model of the soil, a Hardening Soil Small model was used [33]. The parameters of this model associated with the soil are shown in Table 2. Four soft soils are considered, all with the same wave propagation speed of C_s =80 m/s but with a different plastic index (PI) since this has a strong influence on non-linear critical speed [16].

Table 2 – Material properties adopted for the HSSmall model

Element	E_0 (MN/m^2)	E_{50} (MN/m^2)	E_{oed} (MN/m^2)	E_{ur} (MN/m^2)	ϕ (º)	c (kN/m^2)	Ψ (º)	$\gamma_{0.7}$
Embankment (PI 0)	200	35	35	70	45	5	10	7.5×10^{-5}
Soft soil (PI 70)	30	1.3	1.3	4	0	50	0	1.4×10^{-3}
Soft soil (PI 50)	30	1.3	1.3	4	0	50	0	9.7×10^{-4}
Soft soil (PI 30)	30	1.3	1.3	4	0	50	0	6.7×10^{-4}
Soft soil (PI 15)	30	1.3	1.3	4	0	50	0	3.6×10^{-4}
Stiff soil	212	40	40	80	35	5	10	2.4×10^{-4}

Only a static analysis is required to apply the simplified methodology, by means of which the average static octahedral shear strain in depth is determined for an axle load of 180 kN (Figure 14a). As expressed previously the dynamic octahedral shear strain can be estimated using the dynamic amplification function for the soil (Ω_s). For that purpose, equation (7) needs is corrected using coefficients SR and TR:

$$SR = \frac{1}{\sqrt{\frac{80}{200}}}$$

$$TR = 1 + \frac{1}{\sqrt[3]{\left(\frac{1}{8}\right)^2}} \tag{8}$$

Converting the non-dimensional amplification function for the soil ($\overline{\Omega}_s$) using the coefficients SR and TR, gives rise to the dynamic amplification function expressed in Figure 14b. Therefore the dynamic octahedral shear strain is estimated by multiplying the static octahedral shear strain (Figure 14a) by the dynamic amplification function (Figure 14b). A similar procedure is also applied to the embankment itself, but using the dynamic amplification functions for the embankment (Ω_E).

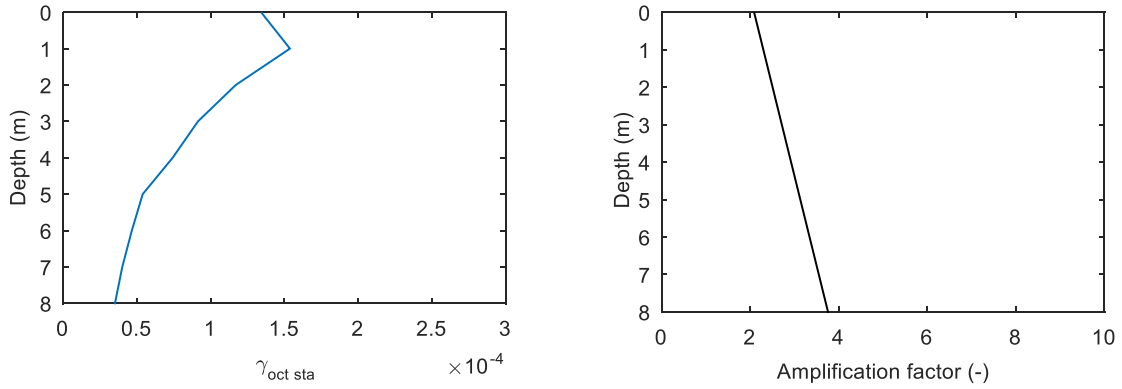

a) b)

Figure 14 – Static octahedral shear strain of the soil (a) and Amplification factor (b) for validation case in slab track

Using the dynamic octahedral shear strain, the degraded properties are calculated for layers with 1m thickness, to better discretize the soil degradation pattern. Figure 15 shows the percentage of degradation obtained for the 8m of soft soil and for all PI combinations. With these degraded geotechnical properties, the respective Shear wave speeds are calculated by means of equation (3). Thus, the dispersion curve corresponding to the degraded scenario is obtained, as shown in Figure 16.

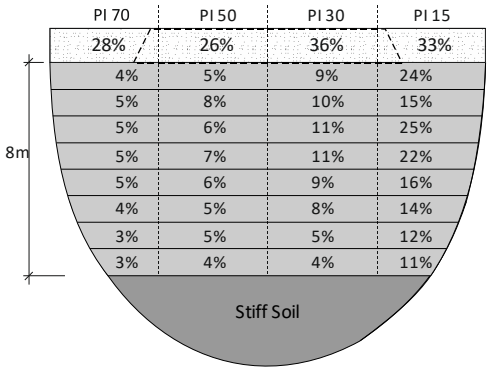

Figure 15 - Degraded properties for all the PI considered (1-G/Go)

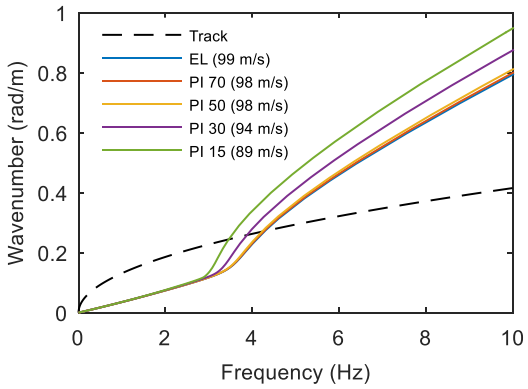

Figure 16 - Dispersion curves for all the PI considered (EL – elastic linear).

The dispersion curves of the degraded soil with high PI hardly vary with respect to the linear elastic scenario, while for low PI the differences are more noticeable. The critical speed values obtained using the methodology are shown in Figure 17, which also compares them with those obtained via the non-linear numerical model. It is observed that the differences between a non-linear model and the simplified methodology are small, with maximum error values of 5% for the high PI's, while for the lowest they are in the range 1-2%.

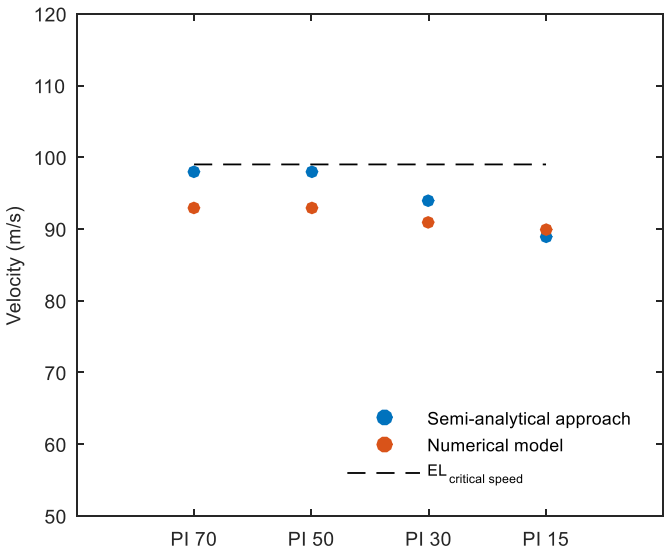

Figure 17 - Critical speed achieved for the scenario with 8 m of soft soil.

The same methodology is also applied to the other geotechnical scenarios previously presented in Figure 9). Figure 18 compares the results obtained using the methodology for the different soft soil thicknesses and those using the non-linear numerical model. The differences for the homogeneous case (Figure 18 c) are small (≈3%), while for thicknesses of 4 and 2m (Figure 18a and Figure 18b) the

differences are marginally larger (≈5.5%). Therefore, the methodology fits the critical speed values from the nonlinear numerical model with reasonable precision.

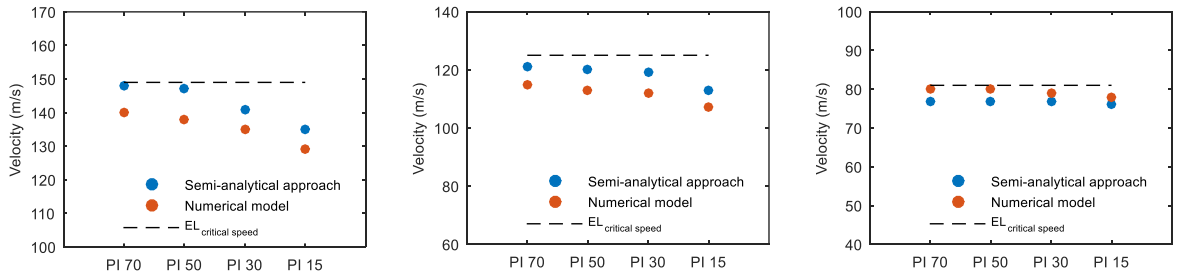

Figure 18 - Critical speed achieved for: a) 2 m of soft soil; b) 4 m of soft soil, c) homogeneous scenario.

It is worth noting that when the PI is low (PI<30), the differences found between the methodology and the non-linear numerical model are smaller than for large PI. This fact can be justified by taking into account that in the dispersion curve method, the degradation computed for a single cross section is assumed as longitudinally invariant. Such an assumption is more realistic for soils with lower PI because the degradation pattern is more widespread both in the longitudinal and vertical directions.

4.2.2 Application case

An application case is considered in order to validate the proposed methodology under different geotechnical scenarios. For this purpose, a new case of soft soil is adopted, characterized by a shear wave propagation speed of 60 m/s. As before, four PI values (15, 30, 50 and 70) and four soft soil thicknesses (homogeneous, 8m, 4m and 2m) are studied. The results obtained for this new geotechnical scenario are shown in Figure 19. The fit for the homogeneous case is good, with maximum differences of 2%. For the case of a thickness of 2m, the differences are somewhat greater, between 3-6%. Even so, for the cases of soft soil thickness of 4 and 8 meters, the differences reach a maximum of 8%. The average difference is 5%, which is reasonable for a simplified methodology that aims to simulate non-linear behavior.

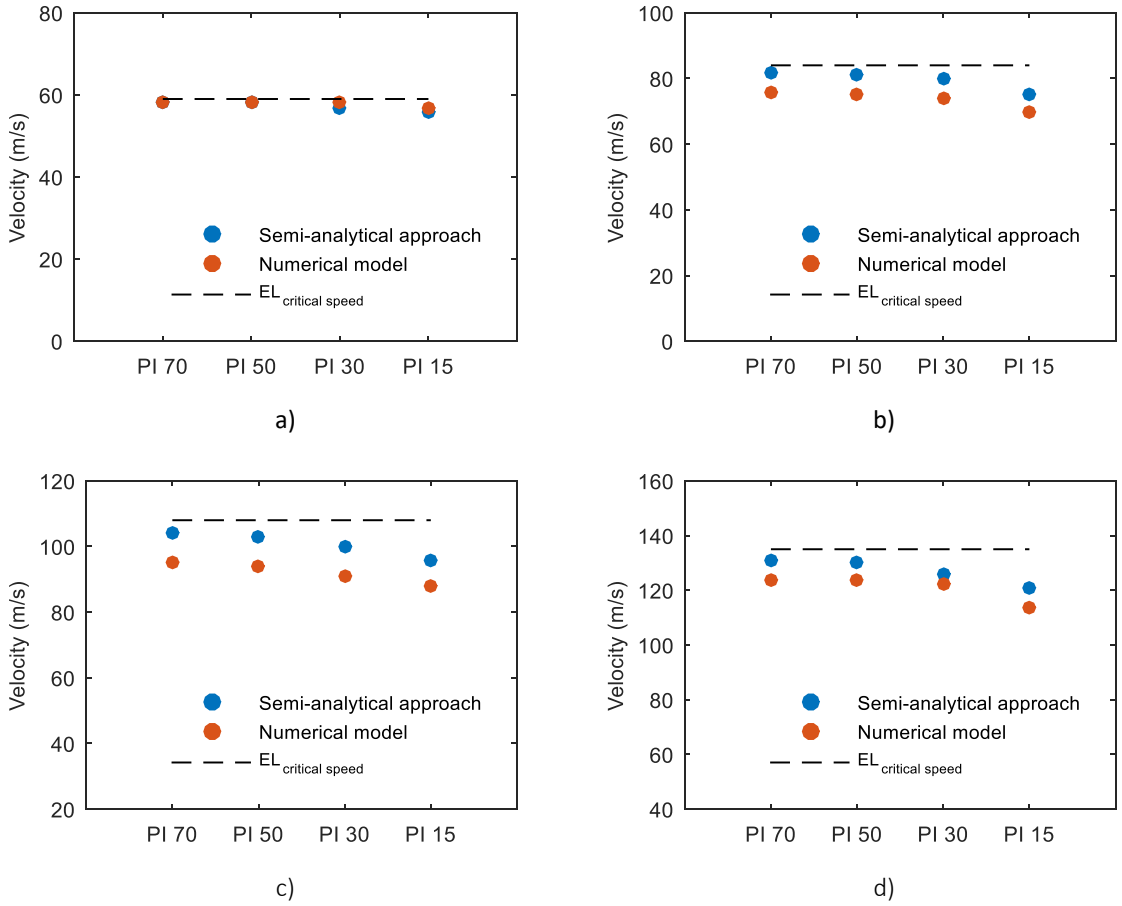

Figure 19 -Critical speed achieved for 60m/s: a) Homogeneous; b) 8 m of soft soil; c) 4m of soft soil; d) 2m of soft soil.

4.3. BALLASTED TRACK

4.3.1. Validation case

Similar to the slab tracks, a reference scenario is first considered to validate the simplified methodology for ballasted tracks. As shown in [16] for certain applications a layered soil can be simplified as a homogeneous one because the critical speed for a ballasted track is determined by the geotechnical properties directly beneath the embankment. Bearing this in mind, a homogeneous geotechnical scenario with 80m/s of shear wave speed is chosen as the validation case (Figure 6). For this geotechnical scenario, the static octahedral shear strain is determined as shown in Figure 20a, with the respective amplification factors shown in Figure 20b. The dynamic amplification function for the soil (Ω_s) is computed by applying the correction SR to the non-dimensional function ($\overline{\Omega}_s$) since the geotechnical profile is a homogeneous one. A similar procedure is applied to the embankment to calculate it's dynamic amplification function (Ω_E) given in Figure 12.

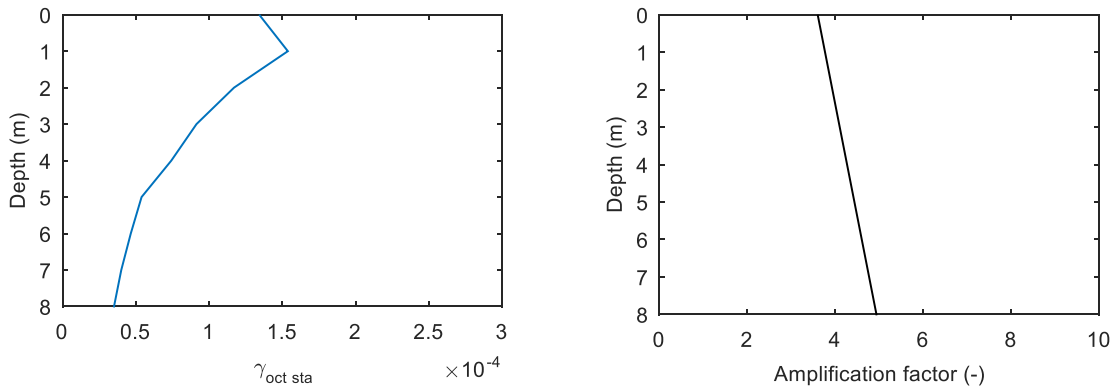

a) b)

Figure 20 – Static octahedral shear strain (a) and Amplification factor (b) for validation case in ballasted track

Following the same analysis strategy as above, the critical speed is computed for all PI values. The results obtained by applying the simplified methodology are expressed in terms of dispersion curves, as can be seen in Figure 21. In contrast to the slab track cases, the ballasted track induces high degradation which leads to a significant reduction in the elastic properties and a lower critical speed. This fact is evident in Figure 21 as the soil dispersion curves for lower PIs show a shift to the left, representing scenarios with more degraded properties. Figure 22 shows the comparison between the results obtained using the simplified methodology and the numerical one. As can be seen, the critical speed predicted is similar to that obtained using the numerical model, with an average error of 1.16%.

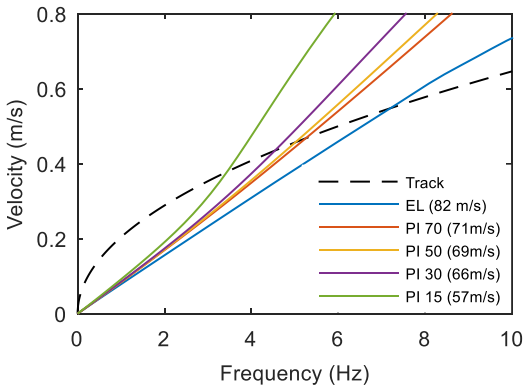

Figure 21 - Dispersion curves for all the PI considered

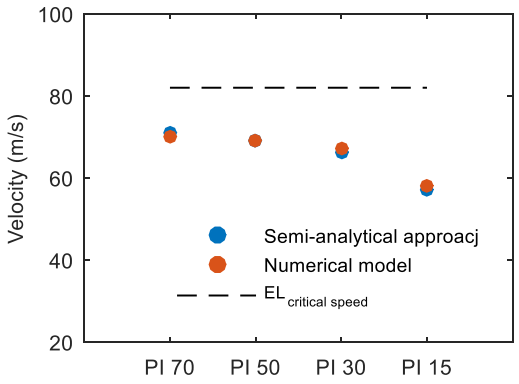

Figure 22 - Critical speed achieved for all the PI adopted

4.3.2. Application case

A new geotechnical profile was evaluated following the same strategy as for slab tracks, by changing the shear wave velocity to 60 m/s. The results achieved for both the simplified methodology and for the numerical model are shown in Figure 23. Again, a good fit between the critical speed predicted by the proposed methodology and the numerical one is achieved, with an average error of approximately

2%. Given that, and taking into consideration all the previous results, it can be concluded that the simplified methodology is capable of accurately predicting the nonlinear critical speed using only the static octahedral shear strain.

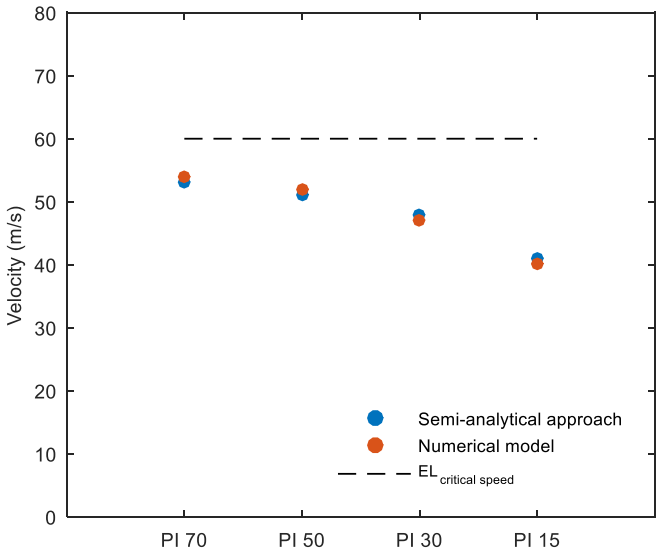

Figure 23 - Critical speed achieved for all the PI adopted.

5 – CONCLUSIONS

This paper proposes a fast-running simplified methodology for the calculation of the non-linear critical speed for high-speed railways. It is based on a novel approach that combines a dispersion curve method with a simplified linear equivalent model based upon shear modulus degradation curves. Using stress fields from a static linear elastic model, a dynamic amplification function is applied to obtain the dynamic strains at the critical speed. Using this and through an iterative process based on a simplified linear equivalent approach, the average degraded properties of the ground are obtained, thus constructing new degraded soil dispersion curves. The critical speed is then the intersection of the degraded dispersion curve and the bending dispersion curve of the track. To achieve this, a novel non-dimensional dynamic amplification function concept is presented for the soil, which can be applied to slab and ballasted tracks in any geotechnical scenario. The function considers two conversion coefficients related with the thickness of soft soil and the stiffness contrast between soft soil and embankment.

The proposed methodology has been validated both for slab and ballasted tracks, varying both the elastic properties of the soil as well as PI and thickness. Comparing the results of the proposed methodology with a 3D non-linear numerical model, acceptable accuracy is observed, with errors

below 5%. In particular, the ballasted track shows negligible differences (≈1%) regardless of the PI of the soil. Regarding the slab track, it shows differences ≈5%, with a better fit when the PI of the soil is low. reason for this difference between track types is because for ballasted tracks the degradation of geotechnical properties is more pronounced than in slab tracks, causing a more widespread degradation both in the embankment and soil. In the slab track, the degradation is less widespread causing the simplified methodology, when working with average degradation properties for layers of 1 m thickness, to have a lower degree of accuracy.

APPENDIX

DISPERSION RELATION OF THE GROUND

For a ground in free vibration conditions, its dispersion behaviour can be achieved by determining the real roots of the dispersion equation. Following the transfer matrices formulation proposed by Sheng et al. [34], the dispersion equation, which establishes a relation between displacements (u_0) and pressures (p_0), is given by:

$$\left([R][S]^{-1}[T_{21}]-[T_{11}]\right)\{\tilde{u}_0\}=\left([T_{12}]-[R][S]^{-1}[T_{21}]\right)\{\tilde{p}_0\} \tag{A1}$$

In order to obtain non-zero values in the above equation, the following equation needs to be satisfied:

$$\det([K(0,k_3,\omega])=0 \tag{A2}$$

where $[K]$ corresponds to the dynamic stiffness matrix:

$$[K(0,k_3,\omega)]=\begin{bmatrix} k_{11}(0,k_3,\omega) & 0 & 0 \\ 0 & k_{22}(0,k_3,\omega) & k_{23}(0,k_3,\omega) \\ 0 & k_{32}(0,k_3,\omega) & k_{33}(0,k_3,\omega) \end{bmatrix} \tag{A3}$$

Thus, for a specific frequency ω, the dispersion curve is obtained by solving the following equation:

$$k_{22}k_{33}-k_{32}k_{23}=0 \tag{A4}$$

DISPERSION RELATION OF THE TRACK

A similar procedure is needed to compute the dispersion curve for a free track in free field condition, where the governing equation is given by:

$$[K]\{u\}=0 \tag{A5}$$

$[K]$ representing the track's stiffness matrix and $\{u\}$ the vertical displacements.

Assuming a Bernoulli-Euler formulation, both the tracks are modelled as a superposition of Winkler beams as shown in Figure 24.

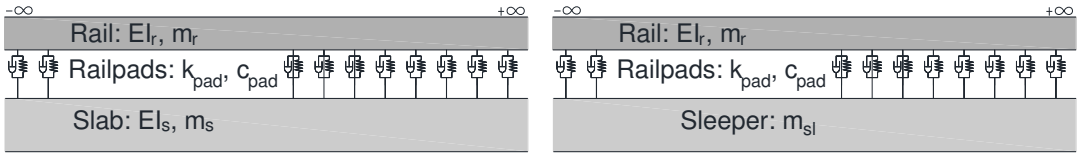

a) b)

Figure 24 – Analytical description of rail tracks: a) slab track; b) ballasted track

The corresponding stiffness matrix can be computed as follows for a slab, and ballast track respectively:

$$[K_{slab}]=\begin{bmatrix} EI_r k_1^4 + k_{pad} - \omega^2 m_r & -k_{pad} \\ -k_{pad} & EI_s k_1^4 + k_{pad} - \omega^2 m_s \end{bmatrix} \quad \text{(A6)}$$

$$[K_{ballast}]=\begin{bmatrix} EI_r k_1^4 + k_{pad} - \omega^2 m_r & -k_{pad} \\ -k_{pad} & k_{pad} - \omega^2 m_{sl} \end{bmatrix} \quad \text{(A7)}$$

For the non-zero solution, the determinant of the matrix must respect the following relation:

$$\det([K]) = 0 \quad \text{(A8)}$$

Thus, the bending dispersion curve for the track is derived by solving equation (A8).

REFERENCES

[1] Y. Gao, H. Huang, C. L. Ho, and J. P. Hyslip, "High speed railway track dynamic behavior near critical speed," *Soil Dynamics and Earthquake Engineering,* vol. 101, pp. 285-294, 2017.

[2] V. Krylov, "Generation of ground vibrations by superfast trains," *Applied Acoustics,* vol. 44 pp. 149-164, 1995.

[3] P. Alves Costa, A. Colaço, R. Calçada, and A. S. Cardoso, "Critical speed of railway tracks. Detailed and simplified approaches," *Transportation Geotechnics,* vol. 2, no. 0, pp. 30-46, 3// 2015.

[4] H. A. Dieterman and A. Metrikine, "The equivalent stiffness of a half-space interacting with a beam. Critical velocities of a moving load along the beam," *European Journal of Mechanics A/Solids,* vol. 15, no. 1, pp. 67-90, 1996.

[5] X. Sheng, C. J. C. Jones, and D. J. Thompson, "A theoretical study on the influence of the track on train-induced ground vibration," *Journal of Sound and Vibration,* vol. 272, no. 3-5, pp. 909-936, 2004.

[6] D. P. Connolly, K. Dong, P. Alves Costa, P. Soares, and P. K. Woodward, "High speed railway ground dynamics: a multi-model analysis," *International Journal of Rail Transportation,* pp. 1-23, 2020.

[7] X. Sheng, C. Jones, and M. Petyt, "Ground vibration generated by a load moving along a railway track," *Journal of Sound and Vibration,* vol. 228, pp. 129-156, 1999.

[8] P. Galvín, S. François, M. Schevenels, E. Bongini, G. Degrande, and G. Lombaert, "A 2.5D coupled FE-BE model for the prediction of railway induced vibrations," *Soil Dynamics and Earthquake Engineering,* vol. 30, no. 12, pp. 1500-1512, 2010.

[9] H. Chebli, D. Clouteau, and L. Schmitt, "Dynamic response of high-speed ballasted railway tracks: 3D periodic model and in situ measurements," *Soil Dynamics and Earthquake Engineering,* vol. 28, no. 2, pp. 118-131, 2008.

[10] H. Chebli, R. Othman, D. Clouteau, M. Arnst, and G. Degrande, "3D periodic BE-FE model for various transportation structures interacting with soil," *Computes and Geotechnics,* vol. 35, pp. 22-32, 2007.

[11] P. Galvín, A. Romero, and J. Domínguez, "Fully three-dimensional analysis of high-speed train–track–soil-structure dynamic interaction," *Journal of Sound and Vibration,* vol. 329, no. 24, pp. 5147-5163, 11/22/ 2010.

[12] J. O'Brien and D. C. Rizos, "A 3D BEM-FEM methodology for simulation of high speed train induced vibrations," *Soil Dynamics and Earthquake Engineering,* vol. 25, pp. 289-301, 2005.

[13] M. A. Sayeed and M. A. Shahin, "Three-dimensional numerical modelling of ballasted railway track foundations for high-speed trains with special reference to critical speed," *Transportation Geotechnics,* vol. 6, pp. 55-65, 2016.

[14] A. El Kacimi, P. K. Woodward, O. Laghrouche, and G. Medero, "Time domain 3D finite element modelling of train-induced vibration at high speed," *Computers & Structures,* vol. 118, no. 0, pp. 66-73, 3// 2013.

[15] J. Fernández-Ruiz, M. Miranda, J. Castro, and L. M. Rodríguez, "Improvement of the critical speed in high-speed ballasted railway tracks with stone columns: A numerical study on critical length," *Transportation Geotechnics,* vol. 30, p. 100628, 2021.

[16] J. Fernández-Ruiz, A. Castanheira-Pinto, P. A. Costa, and D. P. Connolly, "Influence of non-linear soil properties on railway critical speed," *Construction and Building Materials,* vol. 335, p. 127485, 2022.

[17] M. Kaynia, C. Madshus, and P. Zackrisson, "Ground vibrations from high-speed trains: prediction and countermeasure," *Journal of Geotechnical and Geoenvironmental Engineering,* vol. 126, no. 6, pp. 531-537, 2000.

[18] P. Alves Costa, R. Calçada, A. Silva Cardoso, and A. Bodare, "Influence of soil non-linearity on the dynamic response of high-speed railway tracks," *Soil Dynamics and Earthquake Engineering,* vol. 30, no. 4, pp. 221-235, 2010.

[19] K. Dong, D. Connolly, O. Laghrouche, P. Woodward, and P. A. Costa, "Non-linear soil behaviour on high speed rail lines," *Computers and Geotechnics,* vol. 112, pp. 302-318, 2019.

[20] J.-Y. Shih, D. J. Thompson, and A. Zervos, "The influence of soil nonlinear properties on the track/ground vibration induced by trains running on soft ground," *Transportation Geotechnics,* vol. 11, pp. 1-16, 2017.

[21] C. Charoenwong, D. Connolly, P. Woodward, P. Galvín, and P. A. Costa, "Analytical forecasting of long-term railway track settlement," *Computers and Geotechnics,* vol. 143, p. 104601, 2022.

[22] I. Ishibashi and X. Zhang, "Unified dynamic shear moduli and damping ratios of sand and clay.," *Soils and Foundations,* vol. 33, no. 1, pp. 182-191, 1993.

[23] M. Banimahd, P. Woodward, J. Kennedy, and G. Medero, "Three-dimensional modelling of high speed ballasted railway tracks," in *Proceedings of the Institution of Civil Engineers-Transport*, 2013, vol. 166, no. 2, pp. 113-123: Thomas Telford Ltd.

[24] P. K. Woodward, O. Laghrouche, S. B. Mezher, and D. Connolly, "Application of coupled train-track modelling of critical speeds for high-speed trains using three-dimensional non-linear finite elements," *International Journal of Railway Technology,* vol. 4, no. 3, pp. 1-35, 2015.

[25] S. Kramer, *Geotechnical earthquake engineering*. New Jersey: Prentice-Hall, 1996.

[26] B. Hardin and V. Drnevich, "Shear Modulus and Damping in Soils: Measurement and Parameter Effects (Terzaghi Lecture)," *Journal of the Soil Mechanics and Foundation Division,* vol. 98, no. 6, pp. 603-624, 1972.

[27] B. Hardin and V. Drnevich, "Shear modulus and damping in soils: design equations and curves," *Journal of the Soil Mechanics and Foundation Division,* vol. 98, no. 7, pp. 667-692, 1972.

[28] M. Vucetic and R. Dobry, "Effect of soil plasticity on cyclic response," *Journal of Geotechnical Engineering Division,* vol. 117, pp. 89-117, 1991.

[29] J. F. Ruiz, P. J. Soares, P. A. Costa, and D. P. Connolly, "The effect of tunnel construction on future underground railway vibrations," *Soil Dynamics and Earthquake Engineering,* vol. 125, p. 105756, 2019.

[30] N. Yoshida, S. Kobayashi, I. Suetomi, and K. Miura, "Equivalent linear method considering frequency dependent characteristics of stiffness and damping," *Soil Dynamics and Earthquake Engineering,* vol. 22, no. 3, pp. 205-222, 2002.

[31] I. Katayama, K. Ozeki, A. Yamaya, Y. Seshimo, Y. W. Jeong, and H. Suzuki, "Non-linear free-field soil response analysis of a vertical array data," in *Proceedings from the fourth Japan-US Workshop on Earthquake Resistant Design of Lifeline Facilities and Countermeasures for Soil Liquefaction*, 1992, pp. 735-61.

[32] A. Castanheira-Pinto, A. Colaço, J. F. Ruiz, P. A. Costa, and L. Godinho, "Simplified approach for ground reinforcement design to enhance critical speed," *Soil Dynamics and Earthquake Engineering,* Article vol. 153, 2022, Art. no. 107078.

[33] R. B. J. K. Brinkgreve, S.; Swolfs, W.M.; Zampich, L.; Ragi Manoj, N., *Plaxis 2019 User Manuals*. Delft, 2019.

[34] X. Sheng, C. Jones, and D. Thompson, "A theoretical study on the influence of the track on train-induced ground vibration," *Journal of Sound and Vibration,* vol. 272, pp. 909-936, 2004.